with increasing values of x is due to the removal of anisotropy in strength by nonstoichiometry. While the {100} <110> systems in stoichiometric UO_2 are much softer than the {1$\bar{1}$0} <110> systems, this anisotropy disappears in U_4O_9 or $UO_{2.25}$.

References

1. W. VAN LIERDE, to be published.
2. C. HERRING, "Structure and Properties of Solid Surfaces", edited by Gomer Smith (1953).
3. G. WULFF, *Z. Krist.* **34** (1901) 449.
4. W. M. ROBERTSON, *Acta Met.* **12** (1964) 241.
5. B. E. SUNDQUIST, *ibid* 67.
6. W. M. ROBERTSON and P. G. SHEWMON, *Trans. Met. Soc. AIME* **224** (1962) 804.
7. M. B. IVES, *J. Appl. Phys.* **32** (1961) 1534.
8. J. J. BIKERMAN, *Phys. Stat. Sol.* **10** (1965) 3.
9. G. A. WOLFF and J. R. HIETANAN, Condensation and Evaporation of Solids, Proceedings of an Int. Symp., Dayton, 1962 (Gordon and Breach, 1964).
10. O. KNACKE and I. N. STRANSKI, *Z. Elektrochem.* **68** (1956) 816.
11. N. A. GJOSTEIN, *Acta Met.* **11** (1963) 956.
12. T. R. PADDEN and J. BELLE, Paris Conf. on Fuel, 1957.
13. S. TAKAHASHI, T. KUBOTA, H. DOI, and H. UCHIKOSHI, *J. Atom. En. Soc. Japan* **2** (1960) 7.
14. R. G. ROBINS, R. S. WILDS, and B. T. BRADBURY, *J. Nucl. Mats.* **5** (1962) 262.
15. W. VAN LIERDE, R. STRUMANE, E. SMETS, and S. AMELINCKX, *ibid* **5** (1962) 250.
16. P. G. SHEWMON and W. M. ROBERTSON, "Metal Surfaces" (Am. Soc. Metals, 1963) p. 67.
17. R. S. NELSON, D. J. MAZEY, and R. S. BARNES, UKAEA Report AERE-R-4564 (1964).
18. J. K. MACKENZIE and A. J. W. MOORE, *J. Phys. Chem. Sol.* **23** (1962) 185.
19. J. S. NADEAU, *J. Amer. Ceram. Soc.* **52** (1969) 1.
20. A. F. WELLS, *Phil. Mag.* **37** **184** (1946) 605.

Received 19 December 1969
and accepted 19 March 1970

W. VAN LIERDE
Solid State Physics Dept
SCK-CEN
Mol, Belgium

Structure of Undercooled Hypoeutectic Cobalt-Tin Alloys

Earlier work on structure and properties of single-phase undercooled iron and nickel base alloys has shown a substantial modification of dendritic structure [1] and a considerable improvement of ductility [2] with increasing degree of undercooling prior to nucleation of the melt.

In the present study several ingots of hypoeutectic cobalt-10 wt % tin and cobalt-22.5 wt % tin alloys weighing approximately 100 g were solidified with various degrees of undercooling, table I. The experimental procedure used was that described previously [1, 2]. The cooling rate of the specimens after recalescence was 1° C sec^{-1}. Two ingots were surface-chilled [1] and cooled at 300° C sec^{-1}.

There is a substantial change in morphology of the primary cobalt-rich α-phase with increasing degree of undercooling, fig. 1, analogous to that observed in single-phase alloys [1, 2]. Thus, in the non-undercooled specimen the primary phase is equiaxed dendritic surrounded by a lamellar eutectic, fig. 1a. At moderate undercooling, e.g. 75° C, the primary phase exhibits a "cylindrical" dendritic morphology [1] and is also embedded in a lamellar eutectic matrix, fig. 1b. At high undercooling exceeding 170° C the primary phase consists of uniform size spheres embedded in a discontinuous eutectic matrix, fig. 1c. Details of the spherical morphology are shown in fig. 2 which is a photomicrograph of a heavily etched specimen. The internal structure of the spheres is caused by solid state precipitation after completion of solidification during cooling of the ingot. These morphological changes with increasing undercooling are accompanied by a refinement of the dendrite arm spacing in the dendritic specimens and sphere diameter in the specimens of "spherical" morphology. A similar refinement is observed with increasing cooling rate. The explanation of these morphological variations is identical to that suggested for single-phase alloys [1].

Detailed measurements of the volume fraction of the primary phase revealed that it increases with increasing degree of undercooling. These measurements were made using a point counting technique [3]. Table I summarises the variation of weight fraction of the primary α-phase, f_α, versus degree of undercooling. Weight fractions were deduced from measured volume fractions assuming the specific weight of α to be ρ_α = 8.50 g cm^{-3} and that of the cobalt-34 wt % eutectic ρ_E = 8.40 g cm^{-3}.

The variation of f_α with degree of undercooling

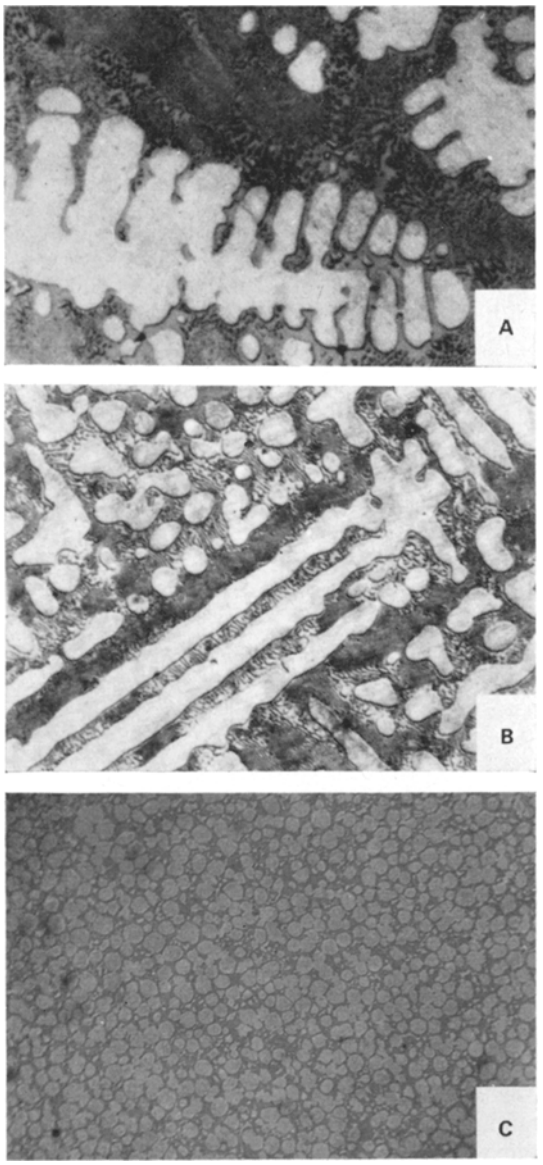

Figure 1 Photomicrographs of cobalt-22.5 wt % tin alloy specimens etched with Rosenhain's reagent (×240). Degrees of undercooling are: (a) 0° C, (b) 75° C, (c) 200° C.

may be used to obtain information about the enrichment in solute of the liquid which remains at the end of recalescence. For this purpose, it will be assumed that the undercooled liquid, nucleated at T_N, recalesces adiabatically to the equilibrium liquidus temperature, T_L. Such an assumption has been shown both experimentally and analytically to be realistic in alloys such as iron-25 wt % nickel and nickel-25 wt % copper

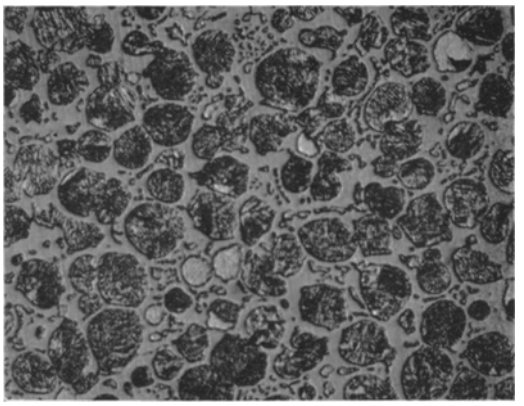

Figure 2 Photomicrograph of cobalt-22.5 wt % tin alloy specimen undercooled 200° C and heavily etched (×516).

for a degree of undercooling up to 200° C [4]. The conservation of thermal energy during recalescence may be expressed by

$$df_S = \frac{\bar{C}_p}{\Delta H} dT \qquad (1)$$

where f_S = weight fraction solid; $\bar{C}_p$ = average specific heat of solid + liquid; ΔH = latent heat of fusion. Assuming $\bar{C}_p$ and ΔH to be independent of temperature, equation 1 may be integrated between ($f_S = 0$, $T = T_N$) and ($f_S = f_{SR}$, $T = T_L$), f_{SR} being the weight fraction solid at the end of recalescence. Hence,

$$f_{SR} = \frac{\bar{C}_p}{\Delta H}(T_L - T_N) = \frac{\bar{C}_p}{\Delta H}\Delta T \qquad (2)$$

where $\Delta T = T_L - T_N$ is the degree of undercooling of the melt prior to nucleation.

In an undercooled specimen, f_{SR} is the weight fraction of primary phase α at the end of recalescence, therefore $(1 - f_{SR})$ is the weight fraction of the remaining non-undercooled liquid which freezes normally with decreasing temperature. Let C^*_{LR} be the solute concentration, assumed uniformly distributed, in this liquid. The weight fraction of α resulting from an equilibrium solidification of the liquid is given by the lever rule as equal to

$$\frac{34 - C^*_{LR}}{30}$$

Thus, the final weight fraction of α is

$$f_\alpha = f_{SR} + (1 - f_{SR})\frac{[34 - C^*_{LR}]}{30} \qquad (3)$$

TABLE I Morphology and weight fraction of primary phase versus degree of undercooling

Degree of undercooling, ΔT (° C)	Morphology of primary phase	Measured weight fraction of primary phase
	Cobalt-10 wt % tin	
0	equiaxed dendritic	0.80
90	cylindrical dendritic	0.86
250	spherical	0.90
	Cobalt-22.5 wt % tin	
0	equiaxed dendritic	0.41
75	cylindrical dendritic	0.50
200	spherical	0.62
250	spherical	0.72

Hence,

$$C^*_{LR} = 34 - 30\,\frac{[f_\alpha - f_{SR}]}{1 - f_{SR}}. \qquad (4)$$

Calculated f_{SR} is plotted versus ΔT in fig. 3. Adopted values of the thermal properties were: $\Delta H = 3210$ cal g-a^{-1} and $\bar{C}_p = 8.5$ cal g-ax° C^{-1} for cobalt-22.5 wt % tin, and $\Delta H = 3448$ cal g-a^{-1} and $\bar{C}_p = 8.74$ cal g-ax° C^{-1} for cobalt-10 wt % tin. These values were deduced from the properties of pure cobalt and tin [5] assuming ideal solutions. Experimental f_α is plotted versus ΔT in fig. 3 using the experimental points reported for cobalt-22.5 wt % tin and cobalt-10 wt % tin in table I. From equation 4, the solute concentration in the liquid at the end of recalescence, C^*_{LR}, may be calculated versus ΔT using the calculated f_{SR} and experimental f_α values given in fig. 3. Results are plotted in fig. 4 and allow the formulation of the following conclusion: for a low degree of undercooling the solute concentration in the liquid at the end of recalescence is practically equal to that of the original melt prior to nucleation of the solid. For a high degree of undercooling it is substantially higher.

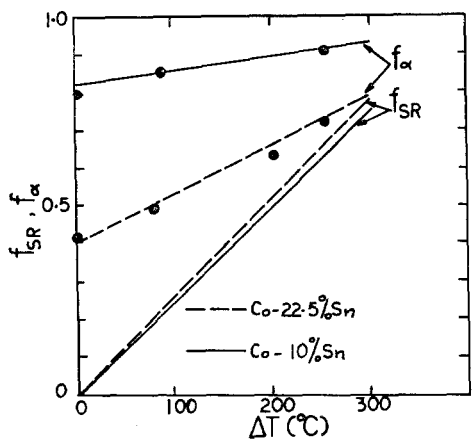

Figure 3 Weight fractions of primary cobalt rich phase at the end of recalescence (f_{SR} calculated on the basis of a simplified recalescence model) and at completion of solidification ($f\alpha$, experimental) versus degree of undercooling, ΔT.

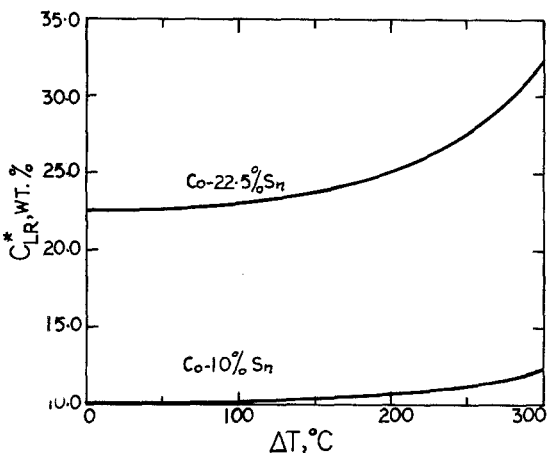

Figure 4 Solute concentration in the liquid at the end of recalescence, C^*_{LR}, versus degree of undercooling prior to nucleation of the melt.

More accurate information may be obtained from elaborate and realistic recalescence models [6], assuming adiabatic recalescence and diffusion or partial remelting of the superheated primary phase.

Acknowledgement

The author would like to thank Dr R. D. Doherty who corrected the manuscript and made helpful suggestions.

References

1. T. Z. KATTAMIS and M. C. FLEMINGS, *Trans. Met. Soc. AIME* **236** (1966) 1523.
2. *Idem, Modern Casting* **52** (1967) 191.
3. J. E. HILLIARD and J. W. CAHN, *Trans. Met. Soc. AIME* **221** (1961) 344.
4. T. Z. KATTAMIS, Sc.D. Thesis, Mass. Inst. of Technology, June 1965.
5. J. F. ELLIOTT and M. GLEISER, "Thermochemistry for Steelmaking", Vol. I (Addison-Wesley Publishing Company Inc., 1960).
6. T. Z. KATTAMIS, to be published, *Z. Metallk.*

Received 6 January
and accepted 3 March 1970

T. Z. KATTAMIS
Department of Metallurgy
Institute of Materials Science
University of Connecticut
Storrs, Conn., USA

A Comparison of Grain-Boundary and Matrix-Crystalline Fracture in Ti-Mo Wires by Scanning Electron Microscopy

Experimental evidence as to the nature of grain-boundaries has been sought for more than a century using, for the most part, indirect methods which normally measure various properties of the material in question rather than the boundary itself. For many years, the grain-boundary was even considered to be a structureless, vitreous layer [1] having an unknown thickness. While the contemporary view of the grain-boundary as a transition from the lattice of one grain to that of the other was seriously considered some 40 years ago [2], this model has only recently been convincingly demonstrated experimentally [3-6]. The structure of grain-boundaries is not completely understood today [6-9], and in particular the boundary thickness is generally not known. A study of fracture uniquely associated with a grain-boundary (as compared with matrix fracture) may be expected to cast light on grain-boundary structure. Such a comparison is, however, difficult to achieve except for specially grown bicrystals, and there seem to be no reports of fracture comparisons of this type in the literature.

During routine operation of an ultra-high vacuum unit, titanium-molybdenum sublimation filaments which failed were observed to have crystallised into large-grained segments with grain-boundaries meeting the wire normal to the axis, as a result of high temperature strain-anneal. It was immediately recognised that because of the embrittlement of the strain-annealed wires, this accidental occurrence presented a good opportunity to study grain-boundary fracture in relation to the fracture of intracrystalline regions along the wire, using the scanning electron microscope. The present study outlines the results of a comparison of fractures in these wires.

High purity Ti-Mo sublimation pump filaments 1.5 to 2 mm in diameter were heated under normal gettering operations in high vacuum using an AC voltage. Under prolonged heating, grains averaging 2 mm in length, with boundaries approximately normal to the wire axis, were formed. Short-time anneals were also performed which produced a fine-grained polycrystalline structure with an average grain size of 0.4 mm.

With a wire section gripped with two pairs of needle-nose pliers, brittle fractures could be induced either at the grain-boundaries of the large-grained wires, or in the grain section between boundaries. The fine-grained wires also fractured in a semi-brittle manner, and served as a means of comparison with the crystalline fractures.

Observations of freshly cleaved surfaces were made in a Cambridge Stereoscan scanning electron microscope operated in the secondary electron mode, using an accelerating potential of 20 kV. Fracture surface orientations were identified using X-ray diffraction techniques.

Spectrographic analysis of various wire samples indicated a molybdenum content ranging from 10 to 14 wt %. 0.004 wt % Mg was observed as the sole impurity element. Electron probe micro-analysis in the region of the grain-boundaries in a number of the samples also indicated a homogeneous alloy, with no noticeable segregation.

Fig. 1 shows a typical length from a Ti-Mo wire sample following crystallisation. It is to be noted that the grain-boundaries are aligned mostly normal to the local wire axis, and there are several examples of grain-boundary sliding. Cleavage fracture within the individual crystals was observed to occur along planes having an angle of approximately 60° to the local wire axis.